Quantitative modeling of threshold instability in β-Ga_2O_3 finFETs through electro-optical investigation

Cite as: APL Mater. 14, 021102 (2026); doi: 10.1063/5.0304986
Submitted: 30 September 2024 • Accepted: 7 January 2026 •
Published Online: 2 February 2026

Manuel Fregolent,[1,a)] Francesco Piva,[1] Carlo De Santi,[1] Matteo Buffolo,[1,2] Wenshen Li,[3] Kazuki Nomoto,[3] Zongyang Hu,[3] Debdeep Jena,[3,4] Huili Grace Xing,[3,4] Gaudenzio Meneghesso,[1] Enrico Zanoni,[1] and Matteo Meneghini[1,2]

AFFILIATIONS

[1] Department of Information Engineering, University of Padova, Padova 35131, Italy
[2] Department of Physics and Astronomy, University of Padova, Padova 35131, Italy
[3] School of Electrical and Computer Engineering, Cornell University, Ithaca, New York 14853, USA
[4] Department of Materials Science and Engineering, Cornell University, Ithaca, New York 14853, USA

Note: This paper is part of the Special Topic on Ultrawide Bandgap Semiconductors.
[a)] **Author to whom correspondence should be addressed:** manuel.fregolent@unipd.it

ABSTRACT

This paper describes the physical origin of V_{TH} instabilities in β-Ga_2O_3 finFETs, based on electro-optical measurements. In particular, (i) we investigated the V_{TH} instability by means of pulsed I_D–V_Gs, demonstrating the existence of an electron trapping process involving border states in the dielectric; then, (ii) we analyzed the charge trapping kinetics at high temperatures, identifying a temperature-dependent mechanism having activation energy of 0.44 ± 0.08 eV; and finally, (iii) we describe a new experimental methodology to investigate the optically stimulated emission of the trapped carriers. The results were employed to develop a quantitative model that identifies, as a root cause for trapping, the presence of a defect band located ~3.3 eV below the conduction band edge of the dielectric layer.

I. INTRODUCTION

Gallium oxide power devices are emerging as candidates for the development of low-cost and high-power transistors and rectifiers targeting the 1–10 kV range.[1,2] Vertical β-Ga_2O_3 devices with different device architectures[3] are currently under study, including current aperture vertical MOSFETs obtained with acceptor implantation[4] or diffusion,[5] trench MOSFETs,[6] and finFETs.[7–9] With respect to the lateral counterparts, vertical β-Ga_2O_3 transistors are preferred for the superior electrical field management, which results in higher breakdown voltages, and for the intrinsic normally OFF operation mode.

Despite the recent advancements in the optimization of the breakdown voltage and ON-resistance, β-Ga_2O_3 devices are still prone to strong V_{TH} instability mechanisms[10–13] usually associated with trapping in oxide or interface traps. Given the ultrawide energy gap of both β-Ga_2O_3 and the dielectric layers, and the consequent presence of very deep-traps (E_A > 0.8–1.0 eV), the analysis of semiconductor/oxide defects is not straightforward and cannot be performed via the conventional temperature-dependent analysis.[10,14,15] In fact, the emission time constant of very deep traps is much longer than the rate window of conventional deep-level spectroscopy apparatus, resulting in an impractical measurement time or in the need of reaching extremely high characterization temperatures.[16]

The goal of this paper is to address this issue by providing a quantitative description and modeling of the traps responsible for threshold instabilities in β-Ga_2O_3 devices. To this aim, we substantially advanced the analysis already reported in Ref. 11 by proposing a novel approach based on high-temperature threshold voltage transients and combined electrical and optical measurements based on a generalization of the deep level optical spectroscopy technique. The procedure was applied on gallium oxide-based finFETs,

and a complete model of the related detrapping transients was obtained.

II. DEVICES UNDER TEST AND PULSED ANALYSIS

The devices under test are vertical β-Ga_2O_3 finFETs[7] [Fig. 1(a)]. A low-doped (2×10^{15} cm^{-3}) 10 μm n^- drift layer was grown by halide vapor phase epitaxy (HVPE) on a highly conductive (001) n^+-β-Ga_2O_3 substrate. Fin channels were defined by electron beam lithography and formed by dry-etching with BCl_3/Ar, followed by HF to recover the damage. Ti/Au drain ohmic contact was formed on the back-side. A 35 nm Al_2O_3 gate dielectric was deposited by atomic layer deposition (ALD), followed by the sputtering of 50 nm Cr as gate metal. Source contacts and field plates consist of Ti/Al/Pt.

A preliminary analysis of the stability of the samples was obtained by performing pulsed-I_D–V_G measurements under gate stress by using a custom experimental setup.[17,18] The devices were biased at a constant quiescent bias (QB) voltage ($V_{G,\ QB}$; $V_{D,QB}$) that was periodically interrupted to perform a short 10 μs pulse to measure the drain current. During the measurement pulse, the drain of the devices were biased at $V_{DS,\ meas}$ = 5 V; under all other conditions, the drain was biased at $V_{D,QB}$ = 0 V to ensure no current flow. The interval between two consecutive pulses was longer than 100 ms; each pulse was averaged 10 times to improve the current resolution of the system: this resulted in a long overall stress time, sufficient to induce a significant trapping in the device. Between the applications of each QB, UV light obtained by a 265 nm LED was shone on the sample for 300 s to restore the pristine state. Typical waveforms are reported in Fig. 1(b). From the results reported in Fig. 1(c), we notice that every positive quiescent bias induces a rightward shift of the I_D–V_G curve, compatible with the trapping of electrons at oxide/interface deep levels, which is also consistent with an earlier report.[19] V_{TH} as function of the applied quiescent bias shown in Fig. 1(d) was extracted by linearly interpolating the I_D–V_G data at a current level of 10^{-4} A.

III. ANALYSIS OF HIGH-TEMPERATURE V_{TH} TRANSIENTS

More insights into the trapping process were obtained by characterizing the kinetics of V_{TH} during stress and recovery experiments in a wide temperature range. This was done through a Keysight B1530 waveform generator and measurement unit, programmed with a custom waveform set, schematically reported in Fig. 2(c). The devices were stressed at a constant $V_{G,str}$ = 3 V for t_{stress} = 1000 s and then recovered for $t_{recovery}$ = 100 s at $V_{G,rec}$ = 0 V. In both phases, drain voltage was kept at 0 V. The stress and recovery phases were periodically interrupted to perform a fast I_D–V_G measurement with a sweep time of 10 μs; at this stage, the drain of the devices was biased at $V_{DS,\ meas}$ = 5 V. The V_{TH} as

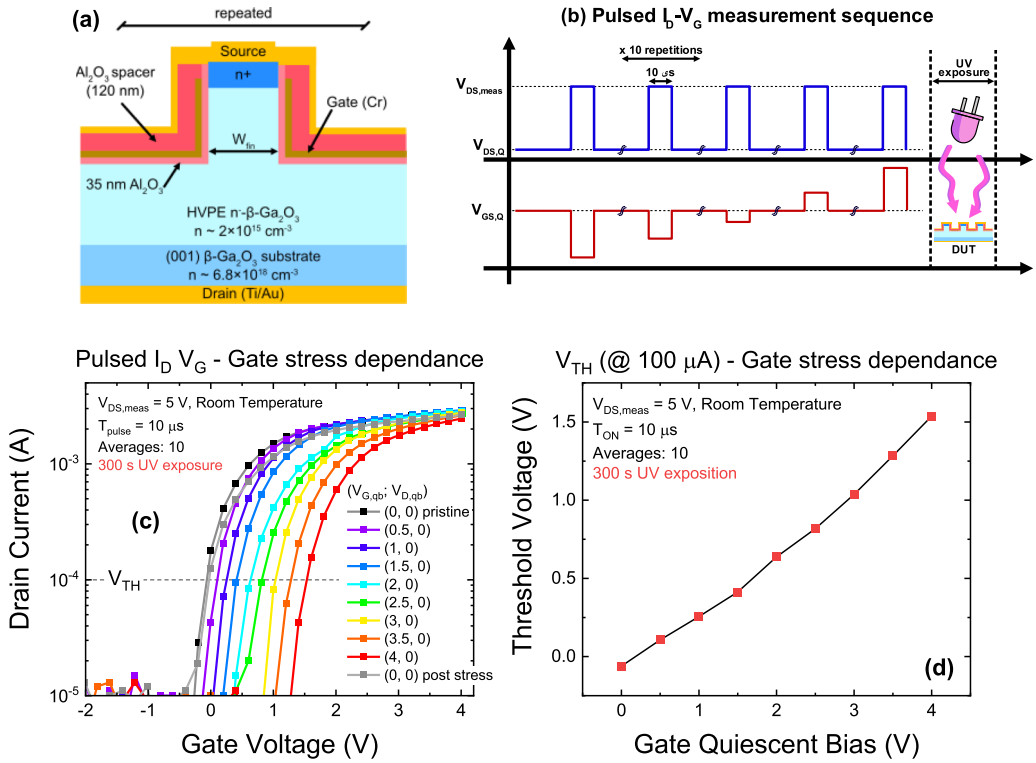

FIG. 1. (a) Schematic structure of the β-Ga_2O_3 finFETs under test; (b) typical waveforms employed in the pulsed I_D–V_G characterization. (c) Pulsed I_D–V_G experiment as a function of a different quiescent bias performed at room temperature (25 °C). (d) V_{TH} extracted by interpolating the experimental data in panel (c) at a current level of 10^{-4} A.

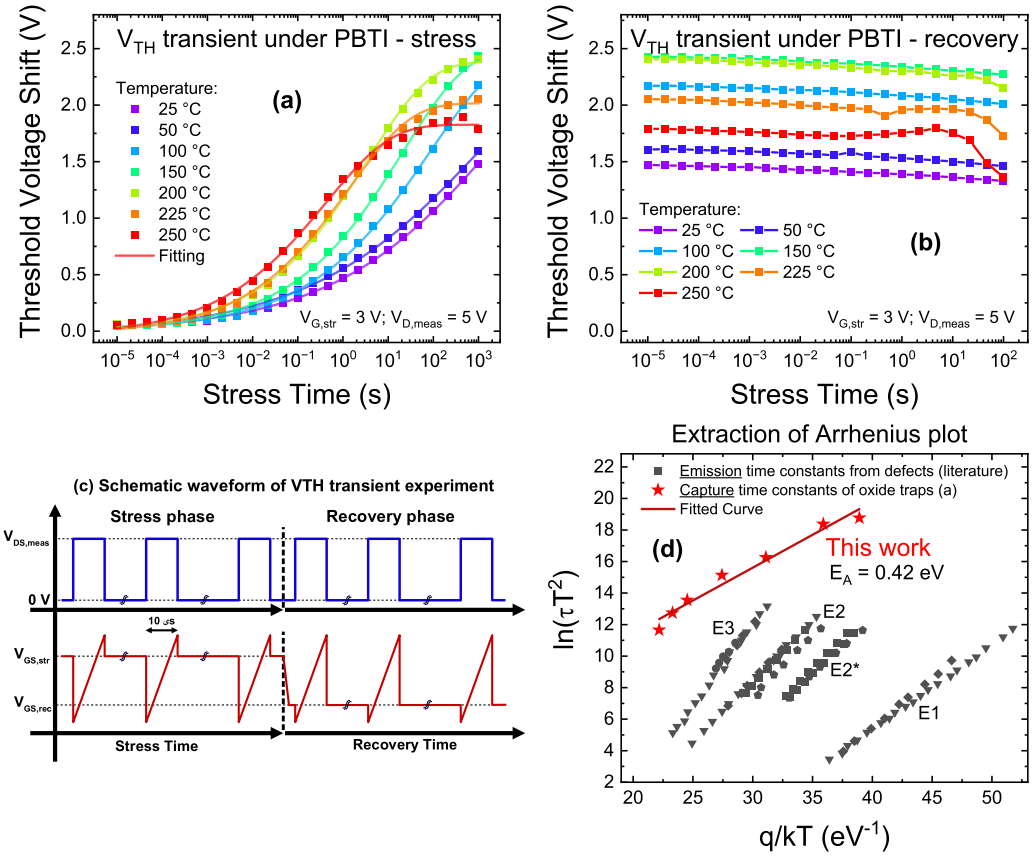

FIG. 2. V_{TH} transients in temperature during a (a) gate stress of $V_{G,stress}$ = 3 V and (b) recovery phase at $V_{G,rec}$ = 0 V. (c) Schematic waveforms of the V_{TH} transient experiment. (d) Arrhenius plot of the capture time constants related to the sample in panel (a) obtained during stress phase is not related to any common defect of β-Ga_2O_3.[16,21]

function of stress and recovery time are reported, respectively, in Figs. 2(a) and 2(b). During stress, V_{TH} shows a thermally accelerated stretched exponential,[20] defined as

$$V_{TH} = V_{TH,0} + A \exp\left[-\left(\frac{t}{\tau}\right)^{\beta}\right], \quad (1)$$

where τ is the time constant of the exponential (depending on temperature as $\tau \sim \exp\left(\frac{E_a}{kT}\right)$) and β is the stretching factor. By fitting the experimental data, we extracted activation energy of 0.42 eV, similar to the one of other traps in β-Ga_2O_3.[16,21,22] However, the levels are not related. In fact, (a) the Arrhenius signature reported in Fig. 2(d) is located in a different region of the plot (indicating a significant difference in terms of time constants); (b) results in Ref. 21 refer to a carrier emission process, whereas data in Fig. 2 are related to the charge capture dynamics. The experiment was then conducted on three other samples, showing similar time constants and Arrhenius plot in the stress phase, leading to extracted average activation energy of 0.44 ± 0.08 eV.

The measured activation energy of 0.42 eV is thus ascribed to a capture barrier that electrons in the accumulation channel have to overcome to be injected and trapped at border traps of the oxide layer [Figs. 5(a) and 6(a)]. The results of tests carried out by keeping the devices at 0 V after stress [Fig. 2(b)] indicate that the charge trapping process is almost completely non-recoverable, even at high temperatures ~200–250 °C. The results, compared to previous literature reports,[10,12] indicate the good stability of the analyzed technology. The findings are also encouraging if compared with early studies on ALD Al_2O_3 on GaN, in which V_{TH} shifts >>1 V, both in MOS capacitors[23] and transistors.[24]

IV. OPTICAL ANALYSIS AND MODELLING

The absence of thermally stimulated recovery shown in Fig. 2(b) is related to the fact that the traps responsible for V_{TH} shift are too deep (in energy) for showing carrier emission. To investigate the related trap-states, we then designed an experimental methodology for optically stimulated emission of trapped carriers.[25] The setup is schematically described Fig. 3(a) and consists of a broad-

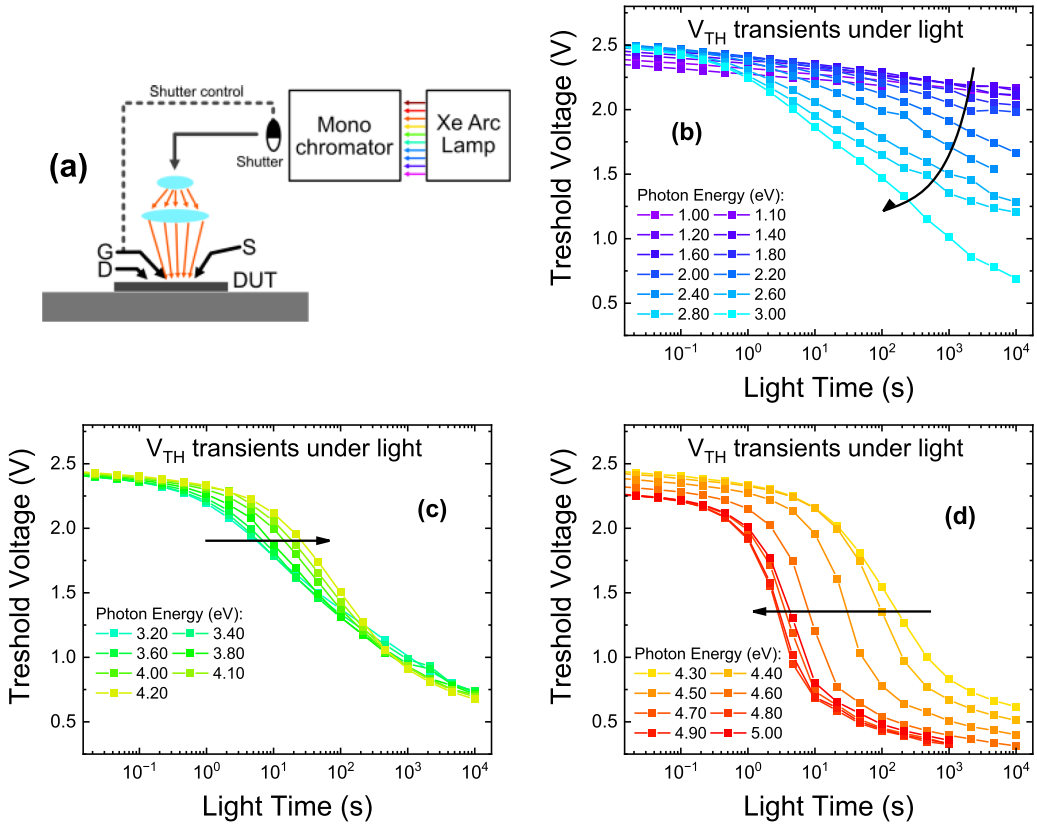

FIG. 3. (a) Experimental setup employed for the detection of optically induced threshold voltage transients. V_{TH} transients under light present three regimes: (b) for low photon energies ($E_{ph} < 3$ eV), we found log-like transients; then (c) for 3.2 eV $\leq E_{ph} \leq$ 4.2 eV, the transients become stretched exponentials; and finally, for $E_{ph} \geq 4.3$ eV, (d) the transients become nearly ideal exponentials with a strong wavelength dependence.

band Xe lamp, a monochromator to select the incident wavelength, a fast mechanical shutter, and suitable lenses to collimate the incident light on the device under test. The control signal for the shutter is obtained by sampling the gate signal (i.e., the shutter opens only during the recovery phase, when $V_G = 0$ V). In this experiment, the devices were stressed for 100 s at $V_{G,str} = 3$ V at room temperature and the carrier emission transient was monitored for 10 ks at $V_{G,rec} = 0$ V under light with the same setup discussed above. The results in terms of V_{TH} kinetic identify four different regimes: (i) for low photon energies $[E_{ph} < 2$ eV, Fig. 3(b)], light does not significantly influence the detrapping process; (ii) for 2 $eV < E_{ph} \leq 3$ eV, the recovery transients are log-like and present a strong wavelength dependence; (iii) for 3.2 $eV < E_{ph} \leq 4.2$ eV, the shape of the transients approaches a stretched exponential, while the time constant remains approximately unchanged; and finally (iv) for high photon energies, the emission transients are nearly ideal and present a strong wavelength dependence.

To analyze the experimental data, we relied on the theoretical background of the deep level optical spectroscopy (DLOS).[16,26] First, we extracted the photoionization cross section of the defects, defined as[16,26]

$$\sigma_o(E_{ph}) = \frac{1}{\Phi_{ph}(E_{ph})\tau(E_{ph})}, \tag{2}$$

where Φ_{ph} is the incident photon flux obtained from a calibration of the optical system and τ is the time constant extracted from a stretched exponential fit. The results shown in Fig. 4(a) confirm the presence of a broad distribution of values of σ_o for $E_{ph} < 4.2$ eV, which is tentatively associated with an energy band of deep levels and a sharp increase in the PCS for $E_{ph} > 4.5$ eV.

Under the hypothesis that the defects in the band are non-interacting, each optical activation energy E_O gives rise to an ideal exponential transient, with amplitude proportional to the defect density $N_T(E_O)$. Now, the V_{TH} shift (which is proportional to the trapped charge) is obtained by integrating the contribution of different defects within the energy gap, following the approach proposed by Modolo *et al.* for thermal emission from defect bands,[20]

$$\Delta V_{TH}(t) \propto n_T(t,\ E_{ph}) = \int_{E_V}^{E_C} N_T(E_O)\left[1 - e^{-\frac{t}{\tau(E_O,\ E_{ph})}}\right] dE_O. \tag{3}$$

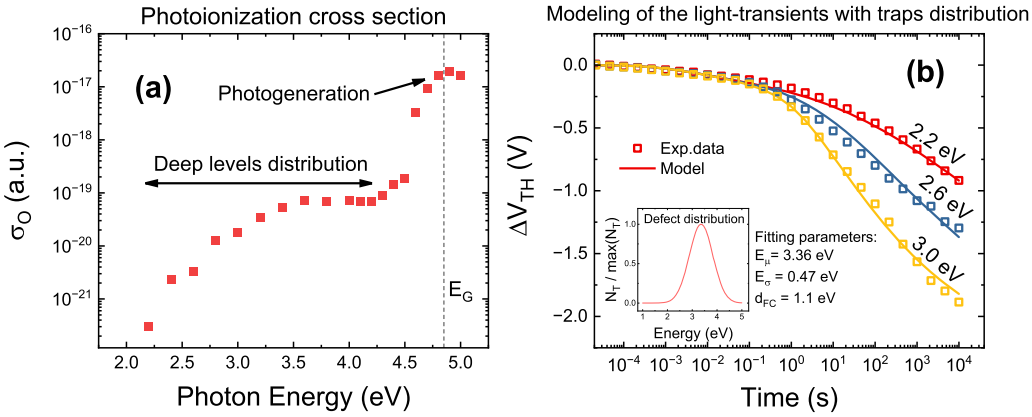

FIG. 4. (a) Photoionization cross section extracted from the optical emission transients according to Eq. (2); (b) numerical simulation of the optical emission transients according to the model in Eq. (3), in which the optical time constants are extracted according to the Passler model.

The time constant of the transients $\tau(E_{ph})$ are then calculated according to Eq. (2), where the photoionization cross section σ_O is estimated from the Pässler model,[27] as a function of the optical activation energy E_O, the Franck–Condon shift d_{FC}, the incident photon energy E_{ph}, and temperature T,

$$\sigma_O(E_{ph}, T) \cong \frac{K}{h\nu\sqrt{2\pi d_{FC}\varepsilon \coth\left(\frac{\varepsilon}{2k_BT}\right)}} \times \int_0^\infty \frac{E_K^{\frac{3}{2}}}{(E_K + E_O - d_{FC})^2} \times \exp\left[-\frac{E_{ph} - E_O - E_K}{2\, d_{FC}\, \varepsilon \coth\left(\frac{\varepsilon}{2k_BT}\right)}\right] dE_K. \quad (4)$$

The model was implemented numerically in MATLAB, and the defect parameters were fitted by means of an optimization algorithm following the approach discussed in Ref. 28 for a subset of the experimental data (2.2, 2.6, and 3.0 eV). The photon energies selected for the optimization algorithm were meant to represent three particular experimental trends: 2.2 eV represent the "strongly stretched/log-like" transients, 3.0 eV is one of the first energies in which we notice an exponential behavior, and 2.6 eV is in between the latter two. The results indicate that the defect distribution that better reproduces the experimental data is a Gaussian distribution, centered at E_μ = 3.36 eV, with standard deviation E_σ = 0.47 eV, and d_{FC} = 1.1 eV [Fig. 4(b), inset]. In this simplified model, we considered that the entire defect band has a constant d_{FC}, as reported in the generalized configuration coordinate diagram in Fig. 5(a); this assumption is valid because d_{FC} does not change substantially for defect with the same origin. The model could be, in principle, extended to consider a generical energy-distribution of the defects and a variable Frank–Codon shift, but this approach was not followed to avoid possible over-parameterization and to simplify the discussion.

The model can be represented with the generalized configuration coordinate diagram reported in Fig. 5. The electrons in the

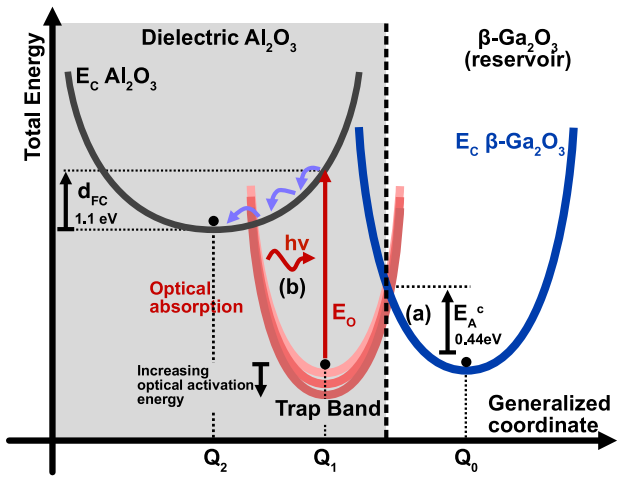

FIG. 5. Simplified configuration coordinate diagram of the (a) trapping and (b) optical detrapping processes.

accumulation channel in the β-Ga_2O_3 layer acts as an electron reservoir,[29] which are then injected into the trap band in the oxide layer with a capture barrier of 0.44 eV that corresponds to the energy that the electrons have to acquire to reach the intercept between the two parabolas. Then, during light illumination, the electrons can be excited in a vertical transition from the defect band to the conduction band of the oxide.

The onset of the fourth regime for the high energy range ($E_{ph} \geq 4.3$ eV) is correlated with the optical ionization of the level E8[16,21,30] in β-Ga_2O_3; therefore, we suggest that this regime is related to the photogeneration of holes from the level E8 that are injected into the oxide and eventually recombine with trapped electrons, as shown in Fig. 6(b3).

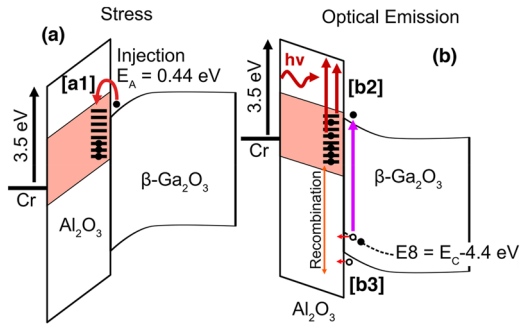

FIG. 6. Macroscopical interpretation of the (a) trapping and (b) optical detrapping processes. When stressed at positive gate voltage, (a1) the electrons in the channel are injected in oxide border states with a thermally assisted process. When the samples are exposed to low-energy photons (b2), they are detrapped through emission to the conduction band of the oxide. High photon energies (b3) induce the photoionization of the E8 trap, with consequent injection of holes in the oxide. Band discontinuity between Cr and Al_2O_3 is from Ref. 11.

V. CONCLUSIONS

In conclusion, we quantitatively investigated the trapping and detrapping processes responsible for threshold voltage instability in β-Ga_2O_3 finFETs with Al_2O_3 gate dielectric. First, we demonstrated that the trapping process is thermally activated, with thermionic barrier energy equal to 0.44 ± 0.08 eV, due to the injection of the electrons in oxide border traps. Then, we developed an advanced technique to analyze the optical-stimulated emission of trapped carriers. The results indicate that the defect band responsible for the trapping process is located at 3.36 eV below the conduction band of the oxide.

ACKNOWLEDGMENTS

This work has been supported by the Wide Bandgap (WBG) Pilot line, which is funded jointly by the Chips Joint Undertaking, through the European Union's Digital Europe programme and Horizon Europe programme, as well as by the participating states Italy, Sweden, Poland, Finland, Austria, France and Germany, under Grant Agreement no. 101183211. This study was carried out within the MOST–Sustainable Mobility Center and received funding from the European Union Next-GenerationEU [PIANO NAZIONALE DI RIPRESA E RESILIENZA (PNRR)–MISSIONE 4 COMPONENTE 2, INVESTIMENTO 1.4–D.D. Grant Nos. 1033 17/06/2022 and CN00000023]. Funded by the European Union. Views and opinions expressed are however those of the authors only and do not necessarily reflect those of the European Union, European Commission or the Chips JU. Neither the European Union, European Commission nor the Chips JU can be held responsible for them

The devices in this study were fabricated under the support of Grant No. AFOSR FA9550-18-1-0529.

AUTHOR DECLARATIONS

Conflict of Interest

The authors have no conflicts to disclose.

Author Contributions

Manuel Fregolent: Conceptualization (equal); Data curation (equal); Investigation (equal); Methodology (equal); Software (equal); Visualization (equal); Writing – original draft (equal). **Francesco Piva**: Conceptualization (equal); Formal analysis (equal); Methodology (equal); Writing – original draft (equal). **Carlo De Santi**: Conceptualization (equal); Formal analysis (equal); Methodology (equal); Writing – original draft (equal). **Matteo Buffolo**: Conceptualization (equal); Formal analysis (equal); Methodology (equal); Writing – original draft (equal). **Wenshen Li**: Conceptualization (equal); Investigation (equal). **Kazuki Nomoto**: Conceptualization (equal); Investigation (equal). **Zongyang Hu**: Conceptualization (equal); Investigation (equal). **Debdeep Jena**: Conceptualization (equal); Funding acquisition (equal); Project administration (equal); Supervision (equal). **Huili Grace Xing**: Conceptualization (equal); Funding acquisition (equal); Project administration (equal); Supervision (equal). **Gaudenzio Meneghesso**: Funding acquisition (equal); Project administration (equal); Supervision (equal). **Enrico Zanoni**: Funding acquisition (equal); Project administration (equal); Supervision (equal). **Matteo Meneghini**: Conceptualization (equal); Methodology (equal); Writing – original draft (equal); Funding acquisition (equal); Project administration (equal); Supervision (equal).

DATA AVAILABILITY

The data that support the findings of this study are available from the corresponding author upon reasonable request.

REFERENCES

[1] A. J. Green *et al.*, "β-Gallium oxide power electronics," APL Mater. **10**(2), 029201 (2022).
[2] C. Gupta and S. S. Pasayat, "Vertical GaN and vertical Ga_2O_3 power transistors: Status and challenges," Phys. Status Solidi A **219**(7), 2100659 (2022).
[3] O. Maimon and Q. Li, *Progress in Gallium Oxide Field-Effect Transistors for High-Power and RF Applications* [Multidisciplinary Digital Publishing Institute (MDPI), 2023].
[4] M. H. Wong, K. Goto, H. Murakami, Y. Kumagai, and M. Higashiwaki, "Current aperture vertical β-Ga_2O_3 MOSFETs fabricated by N- and Si-ion implantation doping," IEEE Electron Device Lett. **40**, 431–434 (2019).
[5] K. Zeng, R. Soman, Z. Bian, S. Jeong, and S. Chowdhury, "Vertical Ga_2O_3 MOSFET with magnesium diffused current blocking layer," IEEE Electron Device Lett. **43**, 1527 (2022).
[6] X. Zhou *et al.*, "Enhancement-mode β-Ga_2O_3 U-shaped gate trench vertical MOSFET realized by oxygen annealing," Appl. Phys. Lett. **121**(22), 223501 (2022).
[7] W. Li, K. Nomoto, Z. Hu, T. Nakamura, D. Jena, and H. G. Xing, "Single and multi-fin normally-off Ga_2O_3 vertical transistors with a breakdown voltage over 2.6 kV," in *2019 IEEE International Electron Devices Meeting (IEDM)* (IEEE, 2019), pp. 12.4.1–12.4.4.
[8] H. C. Huang *et al.*, "β-Ga_2O_3 FinFETs with ultra-low hysteresis by plasma-free metal-assisted chemical etching," Appl. Phys. Lett. **121**(5), 052102 (2022).
[9] K. Tetzner *et al.*, "Enhancement-mode vertical (100) β-Ga_2O_3 FinFETs with an average breakdown strength of 2.7 MV cm^{-1}," Jpn. J. Appl. Phys. **62**(SF), SF1010 (2023).
[10] M. Fregolent *et al.*, "Logarithmic trapping and detrapping in β-Ga_2O_3 MOSFETs: Experimental analysis and modeling," Appl. Phys. Lett. **120**(16), 163502 (2022).

[11]E. Fabris *et al.*, "Trapping and detrapping mechanisms in β-Ga_2O_3 vertical FinFETs investigated by electro-optical measurements," IEEE Trans. Electron Devices **67**(10), 3954–3959 (2020).
[12]Z. Jiang *et al.*, "Experimental investigation on threshold voltage instability for β-Ga_2O_3 MOSFET under electrical and thermal stress," IEEE Trans. Electron Devices **69**(9), 5048–5054 (2022).
[13]H. S. Kim, A. K. Bhat, M. D. Smith, and M. Kuball, "Turn-on voltage instability of β-Ga_2O_3 trench Schottky barrier diodes with different fin channel orientations," IEEE Trans. Electron Devices **71**(6), 3609–3613 (2024).
[14]M. Fregolent *et al.*, "Threshold voltage instability in SiO_2-gate semi-vertical GaN trench MOSFETs grown on silicon substrate," Microelectron. Reliab. **150**, 115130 (2023).
[15]D. V. Lang, "Deep-level transient spectroscopy: A new method to characterize traps in semiconductors," J. Appl. Phys. **45**(7), 3023–3032 (1974).
[16]M. Fregolent *et al.*, "Advanced defect spectroscopy in wide-bandgap semiconductors: Review and recent results," J. Phys. D Appl. Phys. **57**(43), 433002 (2024).
[17]D. Bisi *et al.*, "High-voltage double-pulsed measurement system for GaN-based power HEMTs," in *IEEE International Reliability Physics Symposium Proceedings* (IEEE, 2014), pp. CD.11.1–CD.11.4.
[18]Z. Gao *et al.*, "Dynamic behavior of threshold voltage and I_D–V_{DS} kink in AlGaN/GaN HEMTs due to Poole–Frenkel effect," IEEE Trans. Electron Devices **70**(12), 6256–6261 (2023).
[19]W. Li, K. Nomoto, Z. Hu, D. Jena, and H. G. Xing, "ON-resistance of Ga_2O_3 trench-MOS Schottky barrier diodes: Role of sidewall interface trapping," IEEE Trans. Electron Devices **68**(5), 2420–2426 (2021).
[20]N. Modolo *et al.*, "Trap-state mapping to model GaN transistors dynamic performance," Sci. Rep. **12**(1), 1755 (2022).
[21]Z. Wang, X. Chen, F.-F. Ren, S. Gu, and J. Ye, "Deep-level defects in gallium oxide," J. Phys. D Appl. Phys. **54**(4), 043002 (2021).
[22]K. Irmscher, Z. Galazka, M. Pietsch, R. Uecker, and R. Fornari, "Electrical properties of β-Ga_2O_3 single crystals grown by the Czochralski method," J. Appl. Phys. **110**(6), 063720 (2011).
[23]M. Fregolent *et al.*, "Trapping in Al_2O_3/GaN MOScaps investigated by fast capacitive techniques," in *2023 IEEE International Reliability Physics Symposium (IRPS)* (IEEE, 2023), pp. 1–5.
[24]E. B. Treidel *et al.*, "On the conduction properties of vertical GaN n-channel trench MISFETs," IEEE J. Electron Devices Soc. **9**, 215–228 (2021).
[25]F. De Pieri *et al.*, "Self-induced photoionization of traps in buffer-free AlGaN/GaN HEMTs," IEEE Electron Device Lett. **46**, 369–372 (2025).
[26]A. Chantre, G. Vincent, and D. Bois, "Deep-level optical spectroscopy in GaAs," Phys. Rev. B **23**(10), 5335–5359 (1981).
[27]R. Pässler, "Photoionization cross-section analysis for a deep trap contributing to current collapse in GaN field-effect transistors," J. Appl. Phys. **96**(1), 715–722 (2004).
[28]N. Modolo *et al.*, "Capture and emission time map to investigate the positive VTH shift in p-GaN power HEMTs," Microelectron. Reliab. **138**, 114708 (2022).
[29]T. Grasser, "Stochastic charge trapping in oxides: From random telegraph noise to bias temperature instabilities," Microelectron. Reliab. **52**, 39–70 (2012).
[30]H. Ghadi *et al.*, "Full bandgap defect state characterization of β-Ga_2O_3 grown by metal organic chemical vapor deposition," APL Mater. **8**(2), 21111 (2020).